Modelling the relative stability of carbon nanotubes exposed to environmental adsorbates and air

Modelling the relative stability of carbon nanotubes exposed to environmental adsorbates and air

Amanda S Barnard

School of Chemistry, University of Melbourne, Parkville, Victoria, Australia

E-mail: amanda.barnard@unimelb.edu.au

Abstract

In parallel with the development of technological applications for carbon nanotubes, issues related to toxicology and environmental impact are also under increased scrutiny. It is clear from the available literature that the integrity of future carbon nanotube-based devices, our ability to anticipate failure of these devices, and our ability to manage the toxicological and environmental impacts require a detailed understanding of the stability of pure and functionalized carbon nanotubes under a full range of environmental conditions. Motivated by this endeavour, the present study uses a general thermodynamic model to predict the relative stability of carbon nanotubes exposed to a variety of atmospheric adsorbates, and uses them to examine the stability of nanotubes in air, as a function of the relative humidity. In general the results indicate that the adsorption of a sparse coverage of air is thermodynamically favoured, depending on the humidity, and the stability of small diameter nanotubes may be improved by exposure to humid air.

(Some figures in this article are in colour only in the electronic version)

1. Introduction

Almost 20 years after their discovery [1], carbon nanotubes (CNTs) are still receiving considerable attention as study of their remarkable electronic, metallic, and structural characteristics moves from the realm of nanoscience to nanotechnology [2, 3]. The development of a variety of anticipated applications, such as sensors [4] (including biosensors [5]), tips for scanning probe microscopy [6], electrochemical actuators [7] and batteries [8], is now beginning to be realized. In parallel to these high performance CNT-based nanotechnologies, the toxicology of CNTs is also under scrutiny [9–12], along with the consideration of possible environmental impacts [13–16] and issues surrounding workplace safety [17]. Carbon nanotubes are already being compared to asbestos [17, 18], and exposure of the mesothelial lining of the body cavity of mice to long multi-walled carbon nanotubes has been show to result in asbestos-like, length dependent, pathogenic behaviour [19].

It has been shown that the functionalization of carbon nanotubes can reduce toxicity [20], but the stable binding of the bridging atoms to CNTs is intrinsically linked to the environmental factors such as temperature [21–23]. Clearly, the integrity of future carbon nanotube-based devices, our ability to anticipate failure of these devices, and our ability to manage the toxicological and environmental impacts when the devices are used in certain environments or are discarded, all require a detailed understanding of the stability of pure and functionalized carbon nanotubes under a full range of environmental conditions. The compilation of such a catalogue is an enormous undertaking, however, the most natural starting point must be air and water. The chemical composition of dry air is dominated by nitrogen (78.084% by volume, as N_2) and oxygen (20.9476% by volume, as O_2). Naturally the chemical composition of water is dominated by H_2O, and we may consider humid air (characterized by the relative humidity) as a type of link between the two.

In order to contribute to this effort, the present study outlines a theoretical framework for studying the stability of CNTs in the presence of adsorbates or functional ligands. The method uses a thermodynamic model to examine the relative stability of carbon nanotubes exposed to a variety of atmospheric adsorbates, and uses them to construct a description of nanotubes in air as a function of the relative

(ambient) humidity. In general the results indicate that the adsorption of sparse coverage of air is thermodynamically favoured, depending on the humidity, and the stability of small diameter nanotubes is actually improved by exposure to humid air.

2. Theoretical method

The general thermodynamic model selected for use here is designed to treat carbon nanotubes in the presence of any chemisorbed adsorbate (X) [24]. The model is a simple sum of energetic contributions from C–C and C–X bonds, and the curvature dependent strain energy associated with the CNT tubular structure. The main advantage of this model over alternative (simpler) descriptions is the inclusion of the entire defective region surrounding (and resulting from) the adsorbed atom or molecule, and the energetic contribution of the rehybridization of C atoms contained within this defective region. A detailed description of the model is contained in [24], but briefly the enthalpy of formation per carbon atom ($\Delta H_f^0/N_C$) is expressed as

$$\frac{\Delta H_f^0}{N_C} = \frac{N_C - N_{sp^3}}{N_C} E(sp^2) + \frac{N_{sp^3}}{N_C} \left[\frac{3}{4} E(sp^3) + E_{DB} \right]$$
$$+ \Theta \left[E_b(\Theta, R, X) - E_{DB} + \Delta H_f^0(X) \right] + \Delta H_f^0(C)$$
$$+ \frac{E_s(\Theta, X)}{R^2}. \tag{1}$$

In this expression N_{sp^3} is the number of sp³-bonded C atoms, E_{DB} is the energy of a 'dangling' carbon bond, $E(sp^2)$ and $E(sp^3)$ are the sp² and sp³ cohesive energies, respectively. The 3/4 term arises due to the under-coordination of three-fold coordinated sp³-bonded atoms, rather than from the different number of bonds associated with sp³- and sp²-bonded atoms. $\Delta H_f^0(C)$ and $\Delta H_f^0(X)$ are the experimental formation enthalpies for a carbon atom and the adsorbate, respectively. R is the mean radius of curvature, and finally $E_b(\Theta, R, X)$ and $E_s(\Theta, X)$ are the chemisorption binding energy of X and the strain energy of the nanotube (respectively) which are a function of Θ, the uptake of X (or degree of coverage of X). This has the associated criteria that $0 \leqslant N_{sp^3} \leqslant N_C$, and for a given degree of adsorbate coverage $\Theta = N_X/N_C$, where $0 \leqslant N_X \leqslant \Theta_{max} N_C$. Note that the numerical value of the maximum coverage of X, Θ_{max}, depends upon the adsorption pattern and the extent of the defect resulting from individual adsorbates.

This model may be parameterized for any X by calculating (or measuring) the values of $E(sp^2)$, $E(sp^3)$, E_{DB}, $E_b(\Theta, R, X)$ and $E_s(\Theta, X)$, and via appropriate selection of Θ. An advantage of the model is that when the molecules are chemisorbed, these quantities may be calculated using *ab initio* methods such as density functional theory (DFT). Unfortunately this prohibits the investigation of physisorption, since DFT is unreliable for the calculation of the physisorbed states (which is still relevant to water). Before proceeding, it is also important to point out that since this is a thermodynamic model, it assumes spontaneous chemisorption of all constituents independent of species, and excludes kinetic effects such as reactions at the surface.

3. Computational parameterization

In the present study, all computational parameters included here have been calculated using density functional theory (DFT) within the generalized gradient approximation (GGA), with the exchange correlation functional of Perdew and Wang (PW91) [25]. This has been implemented via the VASP code [26, 27], using a plane-wave basis expanded in real-space (in this case) to a kinetic energy cut-off of 290 eV. This cut-off is low, but is consistent with previous work (that is utilized here) and since this is a comparative study, uncertainties introduced by this cut-off are less than the uncertainties inherent in the fitting procedure (described below). All structures have been pre-relaxed prior to calculation of the various energies, using the linear tetrahedron method (LTM) and ultra-soft, gradient-corrected Vanderbilt-type pseudopotentials (US-PP) [28, 29]. The electronic relaxation technique used here is an efficient matrix-diagonalization routine based on a sequential band-by-band residual minimization method of single-electron energies, with direct inversion in the iterative subspace, whereas the ionic relaxation involves minimization of the Hellmann–Feynman forces, to an energy convergence of 10^{-4} eV. In addition to this, all of the final energies were corrected for the (spin-polarized) energy of the free atomic or molecular species.

To begin with, the parameters for the underlying carbon nanostructure have been previously collected [24] from values obtained in the literature. Using the energies from the sp³-bonded diamond nanowires reported in the literature [30, 31], that employ the same method and convergence criteria, the values of $E(sp^3) = 7.54$ and $E_{DB} = 1.32$ eV have been obtained from the intercept and coefficient (respectively) of a linear fit to the total energy per C atom versus the number of dangling bonds per atom (as shown in [24]). Similarly, by plotting the total energy per C atom for zigzag and armchair CNTs (in the range $n = 4$–12) versus the inverse square of the radius of curvature the values of $E(sp^2) = 7.82$ eV and $E_s(clean) = 2.04$ eV, have been obtained from the intercept and coefficient, respectively, in [31].

A similar procedure is used to parameterize the values of $E_b(\Theta, R, X)$ and $E_s(\Theta, X)$. Due to the large number of adsorbate configurations required to sample structure-space, a sub-set of nanotubes was chosen that sample a range of radii. These are characterized by the (n, m) indices: (5, 0), (9, 0) and (8, 8). Exohedral adsorbates were then chemisorbed onto these CNTs, and the binding energy per adsorbate $E_b(\Theta, X)$ was then determined using the following expression:

$$E_b(\Theta, X) = \frac{1}{N_X} \left[E_{CNT}(N_C, N_X) - E_{CNT}(N_C, 0) - \mu(X) \right], \tag{2}$$

where $E_{CNT}(N_C, N_X)$ is the total energy of the single-walled nanotube (with N_C carbon atoms in the periodic simulation super-cell) adsorbed with N_X atoms or molecules of X, $E_{CNT}(N_C, 0)$ is the total energy of the same single-walled nanotube structure in the absence of adsorbates, and $\mu(X)$ is the chemical potential of X. In the present study the chemisorption energies for oxygen, nitrogen and water were calculated using the molecular chemical potentials from
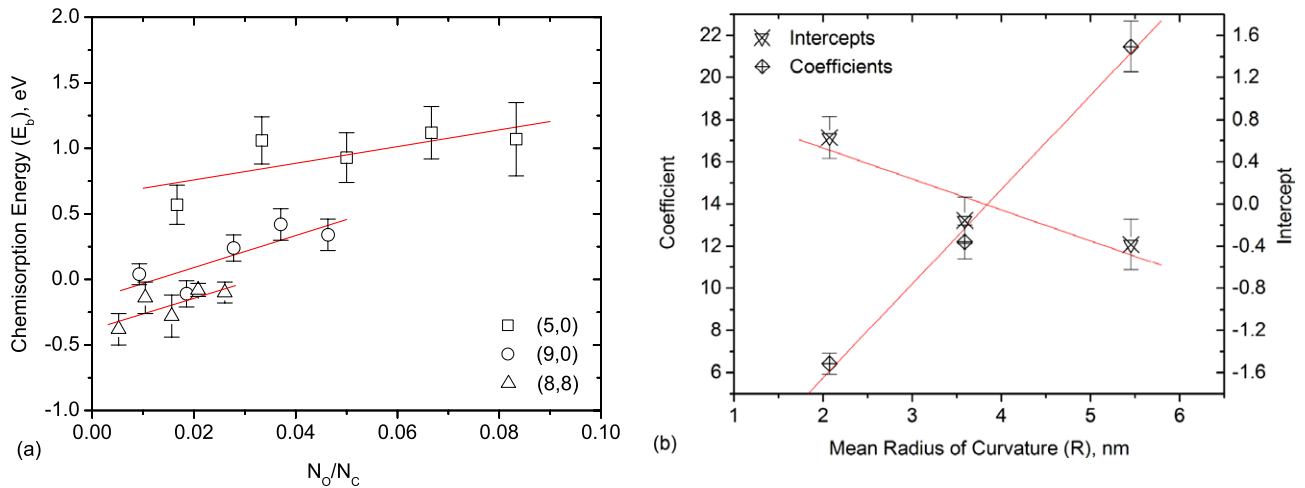
Figure 1. Fitting procedure used to obtain any expression for $E_b(\Theta, R, X)$, using (a) $E_b(\Theta, X)$ for (5, 0), (9, 0) and (8, 8) CNTs, and (b) the coefficients and intercepts from (a) as a function of the mean radius of curvature R. Results correspond to oxygen chemisorption ($X = O$).
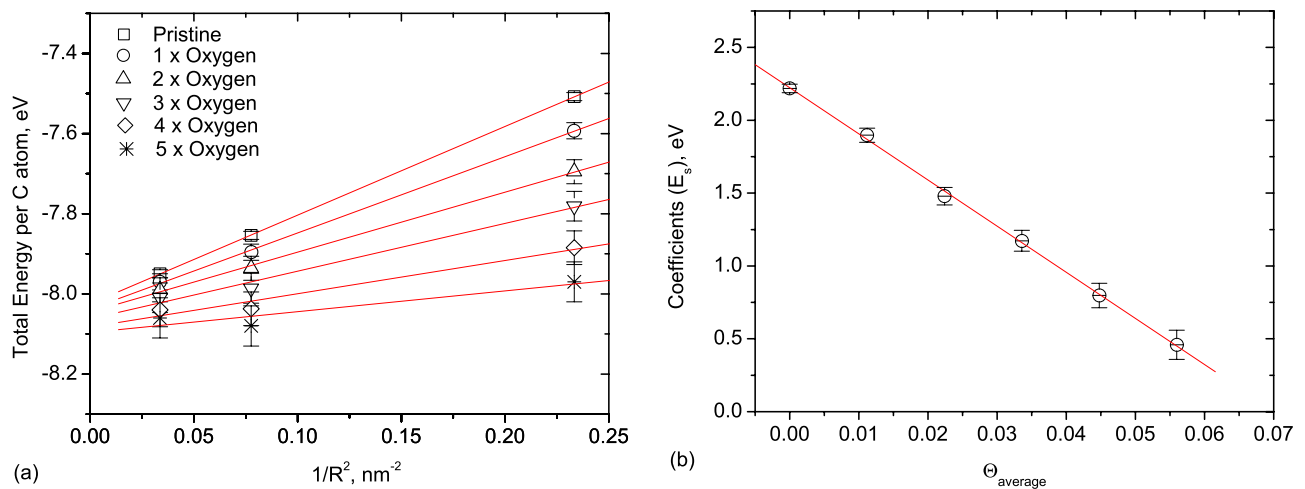

Figure 2. Fitting procedure used to obtain any expression for $E_s(\Theta, X)$, using (a) $E_s(X)$ for (5, 0), (9, 0) and (8, 8) CNTs, and (b) the coefficients from (a) as a function of the coverage of adsorbates Θ.

$\mu(O) = \frac{1}{2}E(O_2)$, $\mu(N) = \frac{1}{2}E(N_2)$ and $\mu(H_2O) = E(H_2O)$ in a vacuum[1]. This means that dissociation of O_2 and N_2 is assumed, since, as stated above, DFT is not suitable for studies of physisorption. In each case, the ground (spin) states were used.

By repeating this procedure for adsorbates clustered in groups of 1, 2, 3, 4 and 5 (as outlined in [24]), $E_b(\Theta, R, X)$ was obtained from linear fits to the coefficients and intercepts of $E_b(\Theta, X)$ over the range of radii. These sets of results for each $E_b(\Theta, X)$ are shown explicitly for $X = O$ in figure 1(a), and the corresponding linear fits to the coefficients and intercepts used to describe $E_b(\Theta, R, X)$ in figure 1(b). Using the same set of computational results, $E_s(\Theta, X)$ was obtained by first calculating $E_s(X)$ from the linear coefficient of the total energy versus the inverse square of the mean radius of

curvature [24], as shown for $X = O$ in figure 2(a). Once again, this was repeated for the adsorbate groups on each CNTs and an expression for $E_s(\Theta, X)$ obtained using linear fits to the coefficients of $E_s(X)$ over the range of Θ, as shown in figure 2(b). Based this fitting procedure, $E_b(\Theta, R, X)$ and $E_s(\Theta, X)$ are condensed down to $E_b(\Theta, R, X) = [aR + b]\Theta + cR + d$ and $E_s(\Theta, X) = e\Theta + f$, with the final set of parameters listed in table 1.

It is important to point out that in each simulation the entire nanotube and adsorbate(s) combination was fully relaxed, so that the adsorbate(s) adopted their low energy
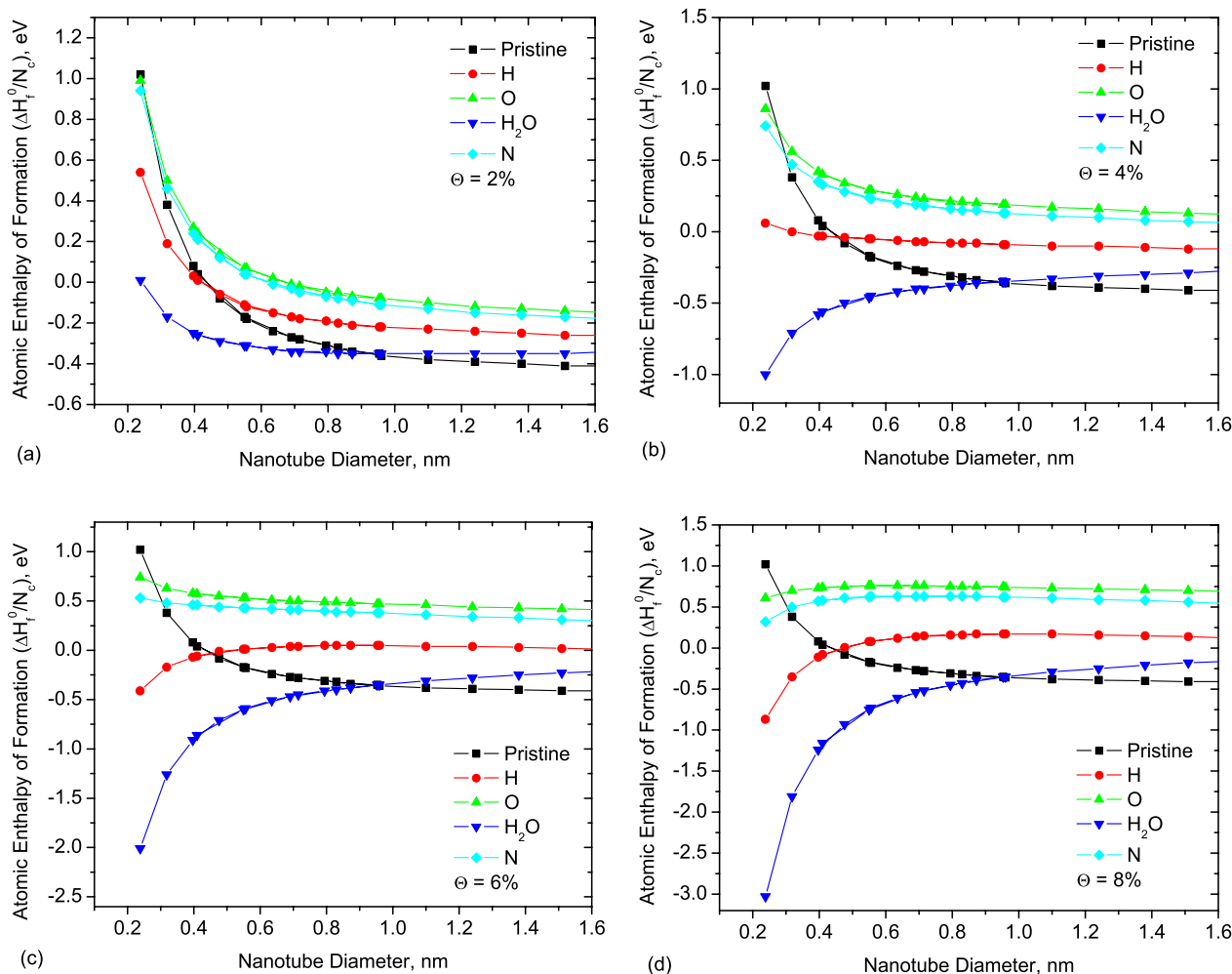
Table 1. Parameterization of $E_b(\Theta, X) = [aR + b]\Theta + cR + d$ and $E_s(\Theta, X) = e\Theta + f$ for $X = O$, N and H_2O. All values are in units of eV.

X	a	b	c	d	e	f
O (from O_2)	3.65	−1.12	−0.29	1.11	−31.67	2.22
N (from N_2)	2.79	3.38	−0.39	−2.22	−35.81	2.26
H_2O (gas)	−4.64	5.44	0.37	−3.08	−74.95	2.08

---

[1] Chemical potentials should be selected (and calculated) so as to best represent the system under consideration. Parameterization with respect to spin un-polarized atomic adsorbates (with $\mu(O) = E(O)$ and $\mu(N) = E(N)$) or with respect to molecular adsorbates in a mixed gas or liquid reservoir will give different results.

Figure 3. Atomic enthalpy of formation for pristine and adsorbate coated nanotubes, with (a) 2%, (b) 4%, (c) 6%, and (d) 8% total coverage of H, O, H_2O and N.

configurations. In the case of N and O this was a bidentate position centred above a C–C bond, and in the case of H_2O it was a monodentate position above a C atom (as previously observed for H adsorption [32]). This means that $N_{sp^3}/N_X = 4$ for N and O, and $N_{sp^3}/N_X = 2.5$ for H_2O (and H).

4. Discussion of results

4.1. Atmospheric adsorbates

Using the model outlined in section 2, and the parameterization described in section 3, the enthalpy of formation per carbon atom $\Delta H_f^0/N_C$ has been calculated for a range of CNTs in the presence O, N and H_2O. These results are compared to pristine CNTs (in a vacuum) in figures 3(a)–(d) for $\Theta = 2\%$, 4%, 6%, and 8%, respectively. Previous results for H [24] are also included for the purposes of comparison, and in each case a random adsorption pattern is assumed, with 20% of adsorbates adjacent to another adsorbate, and 80% isolated with respect to one another.

We can see from figure 3 that the adsorption of water is considerably more favourable than oxygen or nitrogen, even at low Θ. It can also be said that the formation of small diameter

nanotubes is improved in the presence of small quantities of water, and to a lesser extent, hydrogen. This is consistent with recent reports of various (efficient) methods of water-assisted synthesis of CNTs via chemical vapour deposition [33–39] and pyrolysis of organometallic precursors [40]. In addition to this, these results indicate that the formation of ultra-fine nanotubes (such as (4, 0) which is included in figure 3) may become more favourable if N, or possibly O, were present during synthesis. However, one could also argue that these species may also undergo other reactions that have not been explicitly considered here, or that the structure of the defect on such a small nanotube may be inconsistent with the bridging configuration observed in larger diameter structures. It is therefore suggested that quantifying the role of N or O chemisorption in the formation of small diameter nanotubes is an ideal topic for further work, either with or without a catalyst particle.

4.2. Humid air

As mentioned above, the chemical composition of dry air is dominated by N (as N_2) and O (as O_2). Therefore, combining
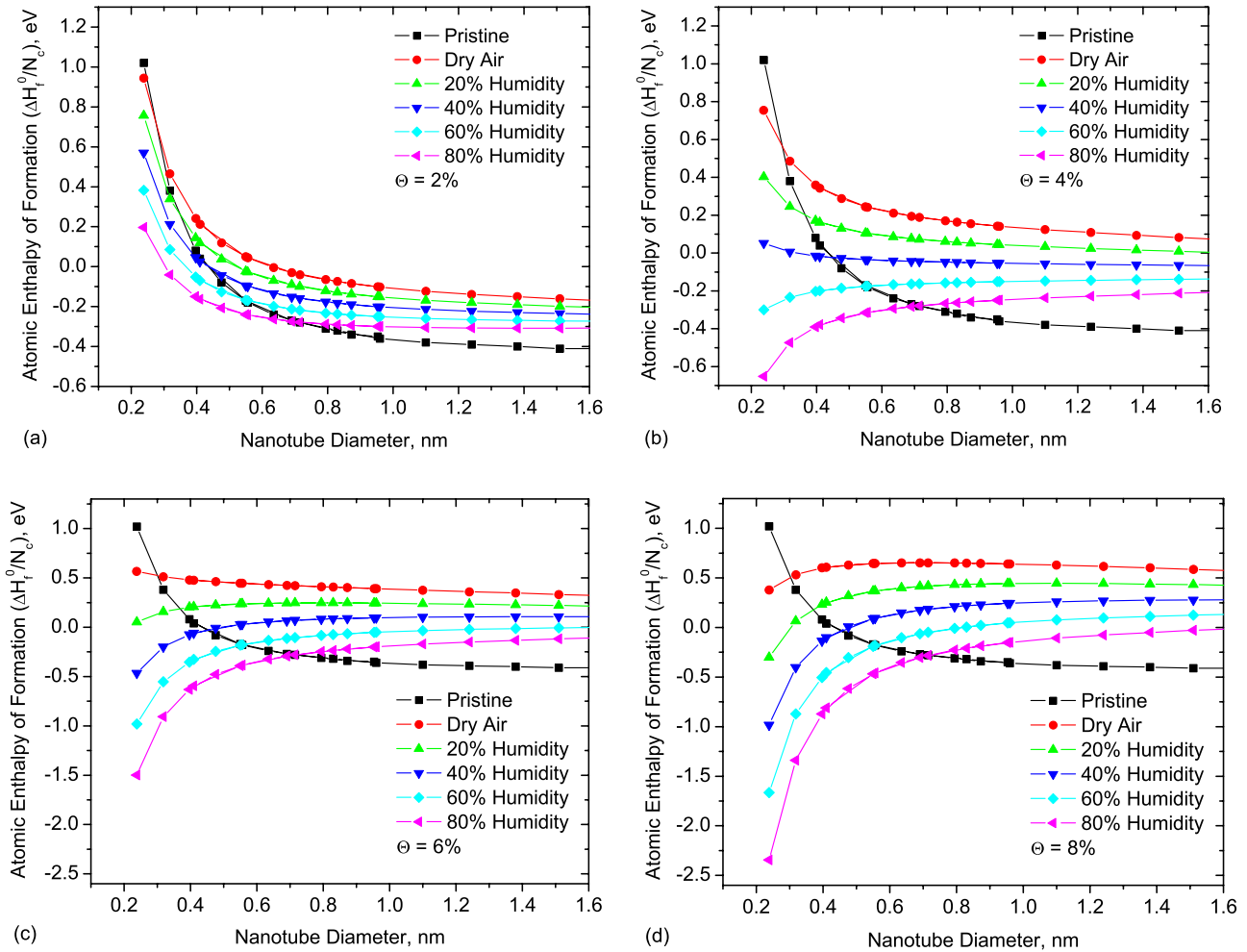
Figure 4. Atomic enthalpy of formation for pristine nanotubes and nanotubes coated with air, with (a) 2%, (b) 4%, (c) 6%, and (d) 8% total coverage of air, with 0% (dry air), 20%, 40%, 60% and 80% relative humidity.

these relative fractions[2] with the parameterizations described above, $\Delta H_f^0/N_C$ has been calculated for a range of CNTs with different coverages of dry air. Since a sparse coverage of water is energetically favourable under ambient condition (with respect to these alternative adsorbates) it is reasonable to assume that the *relative humidity* can be directly translated to the relative fraction of adsorbed water. If water is present, the interaction of water and the nanotube is more likely than the interaction of O or N with the nanotube, but this is not the same as immersing a nanotube in liquid water. It is also important to remember that the present study does not include inter-molecular reactions that may take place in air, nor inter-molecular reactions between adsorbates that may occur on the nanotube wall following individual adsorption events. Pre-adsorption or post-adsorption reactions are beyond the scope of the present study, but could be surmised using standard formation enthalpies for simple molecules in the H/N/O phase diagram.

These results are shown in figure 4, for a range of coverages (Θ) of air with 0% (dry air), 20%, 40%, 60% and 80% relative humidity. Since the choice of Θ matches

those sampled in section 4.1, the results for 100% humidity correspond to the H_2O results in figure 3.

There are two important comparisons to consider when assessing these results. Firstly, there is the direct comparison of the air covered nanotubes with the pristine counterparts. In general, these results show that for diameters below ~0.7 nm the formation of carbon nanotubes is enhanced by humid air, but this critical diameter decreases with decreasing relative humidity. Beyond this size, the formation of nanotubes in a vacuum (pristine structures) is preferred. Secondly, one should also consider the overall thermodynamic stability, with respect to the surrounding environment. At room temperature ($k_B T \approx 26$ meV) $\Delta H_f^0/N_C$ is thermodynamically favourable at $\Theta = 2\%$, irrespective of humidity. As the coverage of air increases (figures 4(a)–(d)), formation in drier air becomes endothermic, and greater degrees of relative humidity are required to ensure nanotube stability. This indicates that these air covered nanotubes are unstable with respect to either disintegration or desorption of certain adsorbates, depending on the relative bond strengths C–X and C–C. If C–X is a stronger bond than C–C, then the nanotube will break given a suitable perturbation, and ultimately disintegrate if the concentration of X is high. Alternatively, if the C–C is

---

[2] The remaining constituents are in low concentrations, and those in this model would not be statistically significant.

a stronger bond than C–X then the desorption of X may be expected rather than disintegration.

Finally, if the relative humidity of the surrounding air is known, these results may also be useful for estimating the likely uptake of air, if we assume that adsorption ceases when Θ is at the point that $\Delta H_f^0/N_C$ becomes endothermic. At this stage it has not been possible to identify enough experimental data to verify this, but as the focus on environmental stability intensifies it is likely that this will change in the near future.

5. Conclusions

Presented here are results of an analytical thermodynamic model predicting the relative stability of single-walled carbon nanotubes chemisorbed with oxygen, nitrogen and water. The model has been parameterized using *ab initio* computer simulations of a range of nanotube structures and adsorption configurations and coverages. The results indicate that the adsorption of water is energetically preferred, and that the formation of small diameter nanotubes is improved in the presence of small quantities of water. The parameterization was also used to model the stability of carbon nanotubes in humid air. These results reveal that the relative humidity of the air surrounding (and interacting with) carbon nanotubes has a strong influence on the overall thermodynamic stability, and the degree of chemisorption that is likely to occur.

Acknowledgments

References

[1] Iijima S 1991 *Nature* **354** 56
[2] Saito R, Dresselhaus G and Dresselhaus M S 1998 *Physical Properties of Carbon Nanotubes* (London: Imperial College Press)
[3] Dresselhaus M S, Dresselhaus G and Avouris P (ed) 2001 *Carbon Nanotubes, Synthesis, Structure, Properties and Applications* (Berlin: Springer)
[4] Kong J, Franklin R N, Zhou C, Chapline M G, Peng S, Cho K and Dai H 2000 *Science* **287** 6226
[5] Sotiropoulou S and Chaniotakis N A 2003 *Anal. Bioanal. Chem.* **375** 103
[6] Wong S, Harper J D, Lansburry P T Jr and Lieber C M 1998 *J. Am. Chem. Soc.* **120** 603
[7] Baughman R H, Cui C, Zakhidov A A, Iqbal Z, Barisci J, Spinks G, Wallace G, Mazzoldi A, De Rossi D, Rinzler A G, Jaschinski O, Roth S and Kertesz M 1999 *Science* **284** 1340
[8] Che G, Lakshmi B B, Fisher E R and Martin C R 1998 *Nature* **393** 347
[9] Zhao Y and Nalwa H S 2006 *Nanotoxicology—Interactions of Nanomaterials with Biological Systems* (California: American Scientific Publishers)
[10] Dumortier H, Lacotte S, Pastorin G, Marega R, Wu W, Bonifazi D, Briand J-P, Prato M, Muller S and Bianco A 2006 *Nano Lett.* **6** 1522
[11] Magrez A, Kasas S, Salicio V, Pasquier N, Seo J W, Celio M, Catsicas S, Schwaller B and Forró L 2006 *Nano Lett.* **6** 1121
[12] Pulskamp K, Diabaté S and Krug H F 2007 *Toxicol. Lett.* **168** 58
[13] Donaldson K, Stone V, Tran C L, Kreyling W and Borm P J A 2004 *Occup. Environ. Med.* **61** 727
[14] Lam C W, James J T, McCluskey R, Arepalli S and Hunter R L 2006 *Crit. Rev. Toxicol.* **36** 189
[15] Barnard A S 2006 *Nat. Mater.* **5** 245
[16] Hyung H, Fortner J D, Hughes J B and Kim J-H 2007 *Environ. Sci. Technol.* **41** 179
[17] Donaldson K, Aitken R, Tran L, Stone V, Duffin R, Forrest G and Alexander A 2006 *Toxicol. Sci.* **92** 5
[18] The Royal Society and Royal Academy of Engineering 2004 *Nanoscience and Nanotechnologies: Opportunities and Uncertainties Report* (London: The Royal Society)
[19] Poland C A, Duffin R, Kinloch I, Maynard A, Wallace W A H, Seaton A, Stone V, Brown S, MacNee W and Donaldson K 2008 *Nat. Nanotechnol.* **3** 423–8
[20] Sayes C M, Liang F, Hudson J L, Mendez J, Guo W, Beach J M, Moore V C, Doyle C D, West J L, Billups W E, Ausman K D and Colvin V L 2006 *Toxicol. Lett.* **161** 135
[21] Durgun E, Dag S, Bagci V M K, Gülseren O, Yildirim T and Ciraci S 2003 *Phys. Rev.* B **67** 201401
[22] Veloso M V, Souza Filho A G, Mendes Filho J, Fagan S B and Mota R 2006 *Chem. Phys. Lett.* **430** 71
[23] Gallo M, Favila A and Glossman-Mitnik D 2007 *Chem. Phys. Lett.* **447** 105
[24] Barnard A S 2006 *Chem. Vapour Depos.* **12** 388
[25] Perdew J and Wang Y 1992 *Phys. Rev.* B **45** 13244
[26] Kresse G and Hafner J 1993 *Phys. Rev.* B **47** R558
[27] Kresse G and Hafner J 1996 *Phys. Rev.* B **54** 11169
[28] Vanderbilt D 1990 *Phys. Rev.* B **41** 7892
[29] Kresse G and Hafner J 1994 *J. Phys.: Condens. Matter* **6** 8245
[30] Barnard A S, Russo S P and Snook I K 2003 *Nano Lett.* **3** 1323
[31] Barnard A S and Snook I K 2004 *J. Chem. Phys.* **120** 3817
[32] Barnard A S, Terranova M L and Rossi M 2005 *Chem. Mater.* **8** 527
[33] Gogotsi Y, Libera J A, Koster van Groos A F and Yoshimura M 2001 *Proc. Joint 6th Int. Symp. on Hydrothermal Reactions (ISHR) & 4th Int. Conf. on Solvo-thermal Reactions (ICSTR) (Kochi, Japan)* pp 350–5
[34] Hata K, Futaba D N, Mizuno K, Namai T, Yumura M and Iijima S 2004 *Science* **306** 1362
[35] Futaba D N, Hata K, Yamada T, Mizuno K, Yumura M and Iijima S 2005 *Phys. Rev. Lett.* **95** 056104
[36] Khavrus V A, Lemesh N V, Gordeichuk S V, Tripol'skii A I, Ivashchenko T S and Strizhak P E 2006 *Theor. Exp. Chem.* **42** 234
[37] Nishino H, Yasuda S, Namai T, Futaba D N, Yamada T, Yumura M, Iijima S and Hata K 2007 *J. Phys. Chem.* C **111** 17961
[38] Jeong S Y, Jeon S H, Han G H, An K H, Bae D J, Lim S C, Hwang H R, Han C S, Yun M and Lee Y H 2007 *J. Nanosci. Nanotechnol.* **8** 1
[39] Patole S P, Alegaonkar P S, Lee J H and Yoo J B 2008 *Eur. Phys. Lett.* **81** 38002
[40] Deepak F L, Govindaraj A and Rao C N R 2006 *J. Chem. Sci.* **118** 9